



Published in final edited form as:

Circ Cardiovasc Imaging. 2017 November ; 10(11): . doi:10.1161/CIRCIMAGING.117.005447.

Multiorgan, Multimodality Imaging in Cardiometabolic Disease

Vidhya Kumar, M.S.¹, Willa A. Hsueh, M.D.^{1,2}, and Subha V. Raman, M.D.¹

¹Ohio State University Davis Heart and Lung Research Institute

²OSU Division of Endocrinology, Diabetes & Metabolism

Abstract

Cardiometabolic disease, spanning conditions such as obesity to type 2 diabetes mellitus with excess cardiovascular risk, represents a major public health burden. Advances in preclinical translational science point to potential targets across multiple organ systems for early intervention to improve cardiometabolic health. Validation in clinical trials and translation to care would benefit from *in vivo* diagnostic techniques that facilitate therapeutic advancements. This review provides a state-of-the-art, multi-modality perspective spanning the multiple organ systems (Figure) that contribute to cardiometabolic disease.

Journal subject terms

imaging; cardiovascular disease; metabolic syndrome

Introduction

Historically, cardiometabolic disease (CMD) has been defined as disorder that encompasses a spectrum of risk factors strongly associated with the development of type 2 diabetes mellitus (T2DM) and that ultimately leads to cardiovascular disease¹. The burden of CMD is high, affecting more than 30% of US adults², and this number is rising in parallel with rates of obesity. Morbidity and mortality due to CMD are ultimately caused by complications associated with cardiovascular disease and T2DM, which together are the leading causes of death in the United States³. While aggressive management of risk factors can improve prognosis in CMD⁴, ongoing discovery of novel mechanistic pathways across various organ systems emphasizes the need for diagnostics that interrogate across relevant systems. Such approaches would facilitate *in vivo* targeting of multiple organs simultaneously to guide therapeutic development and personalize treatment. This review summarizes the pathophysiology of cardiometabolic disease in skeletal muscle, liver, pancreas, adipose tissue, and the microcirculation that collectively impact the heart, forming the basis of multiorgan imaging to assess CMD. Pathogenesis and non-invasive examination of atherosclerosis is excluded from the present discussion, and covered in detail elsewhere.

Address for correspondence: Subha V. Raman, MD, Ohio State University, Division of Cardiovascular Medicine, 473 W. 12th Ave, Suite 200, Columbus, OH USA 43210, Fax 1-614-293-5614, Telephone 1-614-293-8963, raman.1@osu.edu.

Disclosures: SVR receives institutional support from Siemens Healthcare.

Skeletal Muscle

Pathogenesis

Skeletal muscle is the major site of glucose disposal in the body, and plays a crucial role in the development of CMD via: 1) metabolic inflexibility (i.e. inability to use multiple fuel sources) and insulin resistance, 2) intramuscular fat accumulation and 3) impaired mitochondrial oxidative capacity.

Normal skeletal muscle has the potential to draw from both carbohydrate and lipid pools for fuel depending on availability. In metabolically healthy individuals storage and oxidation of glucose is significantly higher in hyperinsulinemic, non-fasting conditions than in fasting states⁵. Furthermore, insulin exposure reduces fatty acid oxidation in healthy individuals. Insulin resistance, due to impaired insulin signaling and glucose transport under abnormal metabolic conditions such as obesity, contributes to inflexibility and increasing reliance on fatty acids as a primary energy substrate. Known CMD causes like chronic over-nutrition and insufficient physical activity adversely affect insulin sensitivity and metabolic flexibility of skeletal muscle⁵.

Metabolic inflexibility and insulin resistance can lead to aberrant mitochondrial oxidative function and ectopic lipid accumulation, including toxic ceramides and diacylglycerol. Increased intra- and extramyocellular lipids (IMCL, EMCL) are associated with CMD, and may indicate an imbalance between fatty acid availability and maximum oxidation potential. Interestingly, ectopic lipid accumulation is not always a pathologic phenomenon. The “athletes paradox” occurs when certain highly trained, metabolically healthy individuals exhibit increased levels of IMCL compared to normal subjects. However, the skeletal muscle of these athletes maintains higher oxidative capacity and is more insulin sensitive than lean, untrained or obese counterparts. Thus, imaging must be interpreted in the context of an individual’s history, physical examination, and other testing⁶. In metabolically-unhealthy individuals, intracellular accumulation of fatty acid oxidation byproducts impairs insulin signaling. The combined effects of insulin resistance and increased reliance on fatty acids leads to mitochondrial uncoupling, an adaptive process that ultimately reduces oxidative phosphorylation capacity⁷. Furthermore, insulin resistant muscle exhibits a greater proportion of glycolytic fibers compared to oxidative, mitochondria-rich fibers⁸.

Mitochondrial Oxidative Capacity

Magnetic resonance spectroscopy tuned to phosphorous (³¹PMRS), an endogenous nucleus found in various high-energy substrates within cells throughout the body, has been used to quantify mitochondrial oxidative capacity and uniquely illuminate biochemistry *in vivo*⁹.

Skeletal muscle³¹PMRS measurements performed *in vivo* with exercise-recovery protocols yield noninvasive quantification of oxidative phosphorylation capacity¹⁰. Such protocols produce an energy imbalance for which increased demand for adenosine triphosphate (ATP) is met through the enzymatic breakdown of phosphocreatine (PCr) through the creatine kinase reaction. Upon cessation of exercise performed to fatigue, the rate of ATP production is dominated by oxidative phosphorylation and represents the maximum *in vivo* capacity of the mitochondria. The post-exercise recovery of PCr can therefore be quantified by the

fitting of an exponential time constant (τ_{PCr}), with shorter values of τ_{PCr} representing greater capacity for oxidative ATP synthesis¹⁰.

Creatine kinase flux

The creatine kinase- catalyzed ATP hydrolysis reaction is fundamental to the production of energy through oxidative phosphorylation. Recently developed magnetization transfer (MT) techniques, which saturate the signal of a nuclei-of-interest and observe the transfer of this saturated signal through chemical exchange, may provide additional insight into skeletal muscle bioenergetics¹¹. Compared to ³¹P MRS methods, MT techniques allow for localized acquisition with relatively high spatial resolution. Furthermore, MT experiments do not require exercise and therefore may be more easily standardized. MT techniques, however, require long scan times and sacrifice feasibility at low field. Long repetition times are required to allow for complete relaxation of the ³¹P nucleus. Incomplete saturation and radiofrequency spillover are issues that are more apparent at low field, although corrections can be introduced into the modified Bloch equations to account for this. However, the combination of low SNR from the low availability of ³¹P in biological systems, combined with saturation and signal homogeneity issues makes the use of high-field systems preferable for MT techniques¹¹.

Metabolite quantification

Carbon 13 (¹³C) MRS offers *in vivo* measurement of various metabolites and their kinetics. To overcome the low natural abundance of ¹³C (~1%) hyperpolarization techniques have emerged to generate ¹³C-tagged metabolites for use as an exogenous contrast agent, increasing SNR by several log-fold¹². Pyruvate, lactate and alanine are important intermediaries in anaerobic and aerobic metabolic pathways that can be examined using hyperpolarized ¹³C MRS. Recent work has demonstrated the feasibility of *in vivo* investigations of skeletal muscle lactate and pyruvate kinetics. However, further work is required to translate these techniques into humans¹³.

Recent advancements in hydrogen MRS (¹H MRS) techniques have enabled quantification of intramuscular metabolites that may change in response to the progression of CMD. Acetylcarnitine (ACC) is an important factor that maintains pyruvate oxidation in the mitochondria. Recent work has demonstrated the feasibility of using long echo time to suppress the lipid signal and detect ACC using ¹H MRS even in overweight/obese subjects¹⁴. Preliminary studies have been completed using ¹H MRS techniques at ultra-high field to quantify skeletal muscle carnosine, an endogenous dipeptide that may improve insulin sensitivity, in response to exogenous supplementation¹².

Fat Quantification

Ectopic intramuscular fat can be quantified non-invasively by ultrasound, computed tomography (CT) or MR. Ultrasound techniques may also identify differences in echogenicity between fat and lean muscle tissue¹⁵. However, intramuscular fat and connective tissue have similar echogenic properties, a significant limitation of this technique¹⁶. The characteristic hypoattenuation of fat by CT signal intensities of -190 to -30 Hounsfield units¹⁷ offers a reliable and simple method for intramuscular fat quantification.

While CT-based fat quantification requires exposure to ionizing radiation, many technical strategies can help minimize dose. Resolution and technique limitations presently preclude CT-based distinction between intra- and extracellular lipids.

MR techniques demonstrate a distinct advantage over other non-invasive fat quantification methods by its breadth. ¹H MRS methods, the current gold-standard for *in vivo* fat quantification, can distinguish between intra- and extracellular fat deposits due to the difference in chemical shift between fat deposits inside and outside of the cell membrane. Fat-water MR imaging methods can quantify and map intramuscular fat. The classic Dixon method of capturing images when fat and water are in-phase and out of phase has been refined for more precise fat quantification.¹⁸

Liver

Pathogenesis

There is a strong link between non-alcoholic fatty liver disease (NAFLD), particularly nonalcoholic steatohepatitis, and CMD. NAFLD, affecting approximately 20% of American adults, describes a range of conditions from ectopic triglyceride accumulation to non-alcoholic steatohepatitis, and is an increasingly common cause of cirrhosis¹⁹.

The precise mechanistic links between NAFLD and CMD remain to be fully elucidated; however, increasing evidence indicates a symbiotic relationship between the two conditions. NAFLD is a known risk factor for T2DM, as it causes hepatic insulin resistance²⁰. Visceral fat accumulation, another characteristic of CMD, contributes to increased hepatic fatty acid levels and intracellular fat accumulation. Furthermore, considerable evidence implicates even simple hepatic steatosis as a predecessor of CMD²¹. Chronic fatty liver, in combination with metabolic syndrome, promotes the development of nonalcoholic steatohepatitis leading to hepatic fibrosis²². Deranged hepatic glucose and lipid metabolism result in increased oxidative stress and potentially disordered mitochondrial function²³. The liver's central role in optimal cardiometabolic health is evident from recent definitions of "metabolically healthy" obese individuals that are predicated on absence of NAFLD²⁴.

Imaging applications

Fat Quantification—Ultrasound is a widely available non-invasive technique for detection of hepatic fat. Steatotic liver demonstrates increased scatter and attenuation sound waves compared to normal liver and produces characteristic qualitative markers such as hyperintense liver, blurry hepatic vessels and poor resolution of the diaphragm. US is the most common method for hepatic fat quantification although its use is limited by low sensitivity and poor penetration in obese individuals²⁵.

CT can be rapidly acquire images to quantify liver fat. However, CT requires exposure to ionizing radiation making it less appealing for serial quantification, and sensitivity may be limited for fat detection below 30%²⁶.

MR can quantify total fat content using imaging methods, and spectroscopy methods can further assay the intracellular fraction. Spectroscopy is typically less widely available both in

instrumentation and expertise. Imaging techniques leverage the difference between in and out-of phase water and fat signals and can produce fat fraction maps²⁵.

Fibrosis quantification—Ultrasound detection of fibrosis with B-mode methods qualitatively assess the liver surface; detection of a nodular liver surface has relatively low sensitivity and is considered reliable for detection of cirrhosis only. Preliminary data suggest high reproducibility and good correlation to histological measures using dual energy CT acquisition and multi-material decomposition to quantify liver fibrosis²⁷; further validation of this technique in prospective trials are warranted. Magnetic resonance elastography is an emerging method involving external placement of a pneumatic driver to generate low-frequency waves. MR elastography techniques may differ between fibrotic and non-fibrotic liver in the context of simple steatosis or steatohepatitis²⁸. However, MR elastography is extremely sensitive to the confounding effects hepatic iron²⁹. Recent improvements to non-contrast multiparametric techniques include T2* correction, which accounts for the T1-shortening effect of hepatic iron that allows for more accurate fibrosis quantification³⁰.

Metabolic quantification—Hepatic glucose utilization can be investigated with positron emission tomography (PET) techniques. ¹⁸F-FDG PET in combination with euglycemic hyperinsulinemic clamp protocols have been used to assess liver glucose utilization. Iozzo et al. demonstrated that in the fasted state hepatic glucose uptake is similar in obese diabetic and normal, healthy-weight individuals. However, glycemic control is inversely related to insulin-stimulated hepatic glucose uptake³¹.

Phosphorous MRS and saturation transfer techniques demonstrate changes in hepatic energetics due to T2DM and obesity. Baseline levels of ATP and inorganic phosphate are lower and rate of ATP turnover slower in individuals with metabolic abnormalities compared to healthy controls³². ¹³C MRS with infusion of labeled acetate can be used to quantify the rate of tricarboxylic acid flux, which is crucial for hepatic fatty acid oxidation³³. Further investigation is required to evaluate this technique in the context of CMD, and to quantify changes due to disease.

Pancreas

Pancreatic beta cell dysfunction is central to a range of metabolic disorders. In type 2 diabetes, hyperglycemia, fatty acids, and oxidative stress cause beta-cell demise so that individuals with impaired fasting glucose have lost 50% of beta cell mass, while around 65% of beta cell mass is lost in frank type 2 diabetes³⁴. Pancreatic fat accumulation impairs beta cell mass and function; intriguing pilot data from Lim *et al.* using MRI-based quantification suggests that marked, short-term calorie restriction lowers pancreatic triglyceride content, normalizes beta cell function, and restores hepatic insulin sensitivity³⁵. Novel molecular probes for use with nuclear imaging techniques, like single photon emission computed tomography (SPECT) and PET, show promise for noninvasive quantification of beta cell mass³⁶. Glucagon-like peptide 1 receptor (GLP-1R) is a protein specifically expressed by pancreatic beta cells, and is a common target for molecular imaging probes. An indium-111 labeled GLP-1R agonist (¹¹¹In-labelled exendin) for use with SPECT imaging has been

developed to quantify beta-cell mass in animals, healthy individuals, and human subjects with beta cell dysfunction³⁷. PET techniques may be preferable to SPECT if increased sensitivity can be offered with lower radiation exposure. However, preliminary PET studies in a large animal diabetes model using a radiolabeled synthetic GLP-1 analog raise toxicity concerns³⁸. Magnetic nanoparticle-tagged GLP-1R agonists have been imaged with MRI, and demonstrate reduced signal in mouse models of diabetes³⁹. Non-invasive quantification of beta cell mass requires further optimization before effective translation to clinical trials.

Adipose Tissue

Pathogenesis

Adipose tissue is the primary caloric reservoir in the body, and it is responsible for maintaining energy homeostasis through regulation of lipid storage and lipolysis in response to environmental requirements. Changes in the ability of adipose tissue to maintain energy homeostasis (i.e. inability to properly store lipids, abnormal signaling or impaired thermoregulation) may precede CMD and further distinguishes metabolic health/disease from normal weight/obesity⁴⁰. The two major types of adipose tissue in humans are: white (WAT) and brown (BAT). The physiological role of WAT is thought to be an insulator and energy reservoir, although recent evidence suggests its role as an endocrine organ as well. A majority of WAT is located in the abdomen, both inside the cavity (visceral) and subcutaneously. Adipokines, adipocyte-secreted cytokines, are secreted by WAT and play a key role in the regulation of energy homeostasis. BAT is highly metabolically active and plays an important role in thermoregulation. Interestingly, while obesity, or excess accumulation of WAT, is associated with CMD it is not necessarily a marker of disease. In fact, a subset of obese individuals are considered “metabolically healthy” because they do not exhibit any other cardiometabolic risk factors, like increased blood pressure or insulin resistance, and do not demonstrate increased risk of CMD compared to normal weight individuals. Interestingly, a primary feature of the metabolically healthy obese subpopulation is the absence of visceral WAT accumulation, which may point to potential mechanisms responsible for CMD⁴¹.

Imaging applications: white adipose tissue

Subcutaneous and visceral WAT mass can be quantified using abdominal imaging techniques such as fat-water MRI, CT, US and dual-energy x-ray absorptiometry⁴². Pathophysiological changes that may occur in subcutaneous WAT include increased inflammation, insufficient tissue oxygenation, and dysregulated endocrine function. Diffuse optical spectroscopy has demonstrated the potential to quantify physiologic changes of subcutaneous WAT (e.g. tissue water fraction and deoxyhemoglobin concentration) during weight loss in obese human subjects⁴³. The phenotype of subcutaneous WAT in CMD, as well as potential changes due to treatment of risk factors, is yet to be investigated.

Imaging applications: brown adipose tissue

BAT is a highly metabolic, insulin sensitive tissue and is therefore well suited to quantification with ¹⁸F-FDG PET. An important caveat to note is that glucose uptake occurs in mainly activated BAT and low FDG uptake may indicate either an absence of BAT or lack

of tissue activation. Cold-induced activation, using cooling vests or rooms, has been used to overcome this limitation although this method is still prone to intra-subject variability. FDG detection of BAT has demonstrated a blunted response in obese subjects compared to lean individuals⁴⁴. Additional PET tracers have been developed for imaging of both active and inactive BAT. Accumulation of radiolabelled tribenzyl phosphonium (¹⁸F-FBnTP) in BAT, which targets changes in mitochondrial membrane potential and proton flux, is inversely proportional to tissue activation. Interestingly, dynamic imaging of ¹⁸F-FBnTP has been used to assess changes due to activation in real-time preclinical models⁴⁵. Further investigation is required to establish the consequences of CMD on BAT function and to evaluate the potential of novel PET tracers in humans.

More recently, MR techniques have been developed for BAT quantification and characterization. BAT, due to differences in lipid storage, vascularity and mitochondrial content, has increased intracellular water content compared to WAT. Dixon MRI techniques can be used to distinguish between BAT and WAT in humans. Franssens et al. demonstrated increased BAT fat fraction in a cohort of patients with CMD using Dixon MRI⁴⁶.

Microcirculation

Pathogenesis

The microcirculation encompasses vessels <150 µm in diameter that support the supply of oxygen and nutrients to tissue as well as stabilize changes in hydrostatic pressure. Altered microcirculatory morphology and function occur in the context of CMD, and accompany pathologies like insulin resistance and hypertension⁴⁷. As insulin exerts a local vasodilatory effect on microvasculature, reduced insulin delivery due to microvascular dysfunction contributes to decreased glucose uptake in skeletal muscle. Furthermore, insulin signaling enhances capillary recruitment promoting more homogenous perfusion and increased glucose uptake in target tissues. Microvascular rarefaction, vessel reduction that significantly increases vascular resistance, occurs with insulin resistance, and hypertension incurs symbiotic detrimental effects on microvascular structure and function⁴⁸.

Imaging applications

CMD-associated microvascular dysfunction can occur in many organs including the eye, skeletal muscle, and heart^{49, 50}. Cutaneous microvasculature may be a particularly appealing target to image the response to cardiometabolic risk-reducing interventions⁵¹. Capillary video microscopy is an optical imaging technique that uses green-spectrum light to illuminate superficial micro vessels in the nail beds. Detectors capture backscattered light and images are reconstructed producing images of capillaries⁵². Contrast-enhanced ultrasound can be used to quantify microvascular recruitment in deeper tissues, like skeletal muscle. Disruption of bubbles with the ultrasound beam and recovery of steady-state can be used to calculate microvascular blood volume and vessel resistance. Meijer *et al.* used such an approach to correlate skin and skeletal muscle microvascular recruitment in healthy individuals to whole-body glucose uptake⁵³. Progressively worse microvascular function has been shown to occur with increased severity of insulin resistance⁵⁴.

Myocardial microvascular function can be accurately quantified with PET⁵⁵. ⁸²Rb PET imaging has been used to demonstrate impaired coronary microvascular function in diabetics without overt cardiovascular disease⁵⁶.

Cardiac Consequences of CMD

Pathogenesis

Across the range of CMD, a number of mechanisms ensue to incur cardiac dysfunction. Aberrant insulin signaling in CMD, both systemic and myocardial, contributes to cardiac dysfunction via altered substrate use, increased oxidative stress and insufficient myocardial perfusion. Subsequent dysregulation of remodeling processes, like cellular hypertrophy, collagen deposition, accumulation of advanced glycaemic end products and ectopic lipid accumulation lead to cell damage, impaired contractile function and diastolic dysfunction⁵⁷. Mitochondrial dysfunction ensuing from CMD affects myocardial energetics may ultimately result in heart failure⁵⁸.

Imaging applications

Echocardiography is the most commonly used technique for non-invasive evaluation of DD⁵⁹. Standard echocardiography techniques quantify the ratio of mitral inflow velocities in early/passive (E) and late/active (A) phases of LV relaxation. A low E:A ratio indicates a greater dependence on active filling to overcome impaired myocardial relaxation. Additionally, lower E' velocity of the mitral annulus during early filling indicates impaired diastolic function. A higher E:e' ratio infers higher LV filling pressures. Increased LV filling pressure and greater dependence on atrial contraction during diastole result in left atrial hypertrophy⁶⁰. Thus, left atrial volume is an additional marker of DD with established prognostic value.

Cardiac magnetic resonance may be used to similarly estimate mitral inflow and annular velocities, whereas unique methods such as tissue tagging offer more direct quantification of myocardial relaxation. Tagged cine superimposes saturation lines or grids onto the imaging plane; their deformation in myocardium over the cardiac cycle is used to calculate systolic and diastolic strain in various directions and components. Cardiac MRS is uniquely capable of quantifying myocardial lipids and interrogating *in vivo* myocardial energetics, which are abnormal in CMD. Wei *et al.* have observed significantly increased myocardial triglycerides in women with CMD using ¹H MRS techniques⁶¹. Using phosphorus spectroscopy, Rider *et al.* demonstrated significantly lower ratio of phosphocreatine to adenosine triphosphate (PCr:ATP) at rest in obese vs. normal-weight individuals, a deficit that improved with weight loss as did measures of LV diastolic function⁶². Using ¹³C cardiac MRS in a rat diabetic cardiomyopathy model, therapy with a pyruvate mimetic has been shown to improve myocardial substrate selection and diastolic function⁶³. ¹³C MRS techniques are also capable of quantifying the effects of anti-diabetic agents on cardiac and hepatic metabolism in preclinical models⁶⁴. Coupled with the distinct capabilities for magnetic resonance-based quantification of myocardial fibrosis, lipid, and energetics, CMR holds significant appeal in the multidimensional, multi-organ characterization of cardiometabolic disease sequelae.

Myocardial substrate utilization varies across the spectrum of CMD, and cardiac PET is uniquely able to visualize glucose uptake *in vivo*. Mobely *et al.* used this modality to demonstrate that a 13-hour infusion of glucagon-like peptide 1 (GLP-1) increases myocardial glucose uptake in lean subjects but not in obese type 2 diabetics⁶⁵.

Multiorgan Approaches in Clinical Trials

Several groups have implemented multiorgan imaging to serially evaluate *in vivo* the effects of therapeutic interventions. Scheuermann-Freestone and colleagues demonstrated one of the earliest multi-organ approaches to detect subclinical metabolic abnormalities in diabetic individuals without evident cardiovascular disease, incorporating exercise ³¹PMRS in skeletal muscle with multimodality cardiac imaging and spectroscopy⁶⁶. Gallagher *et al.* showed reduced mass of the liver and spleen in obese T2DM subjects using whole body T1-weighted MRI in a prospective lifestyle intervention trial, though tissue characterization was not performed to know if mass reduction was effected via reduced fat in these organs⁶⁷. Combining phosphorus and hydrogen cardiac MRS with PET and dobutamine stress echocardiography in a randomized clinical trial of pioglitazone vs. metformin, van der Meer *et al.* demonstrated the potential of a multimodality, multiorgan approach to refine therapeutic strategies for CMD⁶⁸.

Emerging Techniques for CMD Imaging

As insights into CMD mechanisms and therapeutic approaches continue to evolve, emerging imaging techniques offer potential utility in translating these insights to *in vivo* studies in humans. Noninvasive measurement of skeletal muscle oxygen consumption from magnetic susceptibility-based oxygen extraction fraction and arterial spin labeling-based blood flow computations⁶⁹. In the liver, ultrasound-based elastography holds appeal for fibrosis quantification in children and adolescents with nonalcoholic steatohepatitis⁷⁰. Coupled with thermogenic capsaicin-like compounds, near infrared time-resolved spectroscopy holds appeal as a low-cost method to quantify supraclavicular brown adipose tissue⁷¹. Noninvasive interrogation of the cutaneous microcirculation with optical coherence tomography may be enhanced with topical solutions that increase light penetration depth⁷². And in the heart, chemical exchange saturation transfer (CrEST) hold the promise of noninvasive quantification of myocardial creatine kinase metabolism⁷³.

Conclusions

Advances in the non-invasive assessment of cardiometabolic disease across multiorgan sequelae may facilitate earlier detection and improved outcomes. Currently, there are a number of imaging modalities that can be used to detect and quantify various aspects of the disease. With hypothesis-driven approaches targeting key organs, contemporary cardiometabolic imaging affords quantitative, noninvasive, and serial *in vivo* evaluation of disease mechanisms and treatment response. Appropriate techniques warrant greater integration into clinical trials and evidence-guided management of patients with cardiometabolic disease.

Acknowledgments

Sources of Funding: This work was supported in part by the National Institutes of Health (R01 MD007867 to W.A.H. and R01 HL116533 to S.V.R.).

References

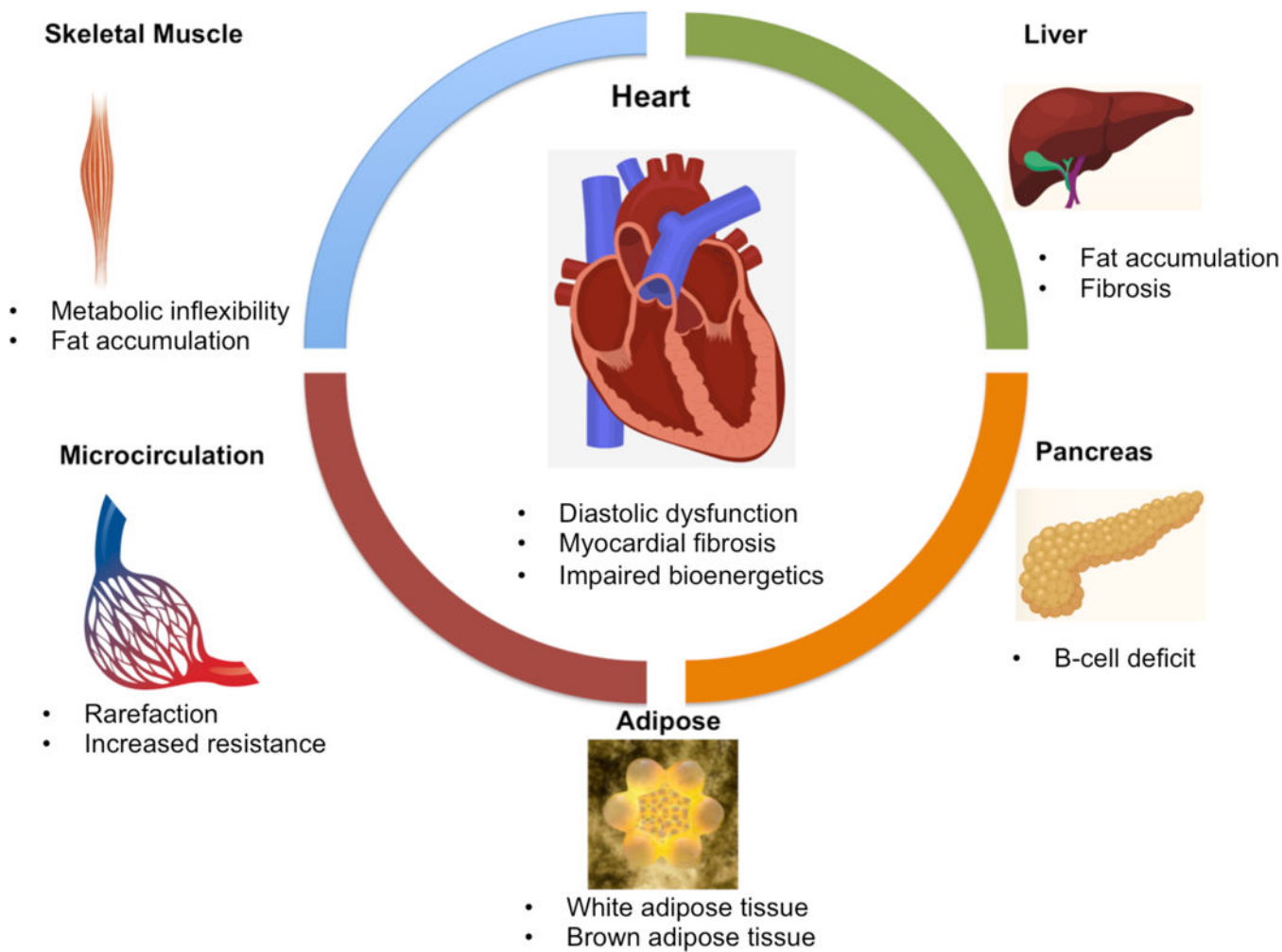
1. Castro JP, El-Atat FA, McFarlane SI, Aneja A, Sowers JR. Cardiometabolic syndrome: pathophysiology and treatment. *Curr Hypertens Rep.* 2003; 5:393–401. [PubMed: 12948432]
2. Mozumdar A, Liguori G. Persistent increase of prevalence of metabolic syndrome among U.S. adults: NHANES III to NHANES 1999–2006. *Diabetes Care.* 2011; 34:216–219. [PubMed: 20889854]
3. Kochanek KD, Murphy SL, Xu J, Tejada-Vera B. Deaths: Final Data for 2014. *Natl Vital Stat Rep.* 2016; 65:1–122.
4. Bozkurt B, Aguilar D, Deswal A, Dunbar SB, Francis GS, Horwich T, Jessup M, Kosiborod M, Pritchett AM, Ramasubbu K, Rosendorff C, Yancy C. Contributory risk and management of comorbidities of hypertension, obesity, diabetes mellitus, hyperlipidemia, and metabolic syndrome in chronic heart failure: a scientific statement from the American Heart Association. *Circulation.* 2016; 134:e535–e578. [PubMed: 27799274]
5. Goodpaster BH, Sparks LM. Metabolic flexibility in health and disease. *Cell Metab.* 2017; 25:1027–1036. [PubMed: 28467922]
6. Brons C, Grunnet LG. Skeletal muscle lipotoxicity in insulin resistance and type 2 diabetes: a causal mechanism or an innocent bystander? *Eur J Endocrinol.* 2017; 176:R67–R78. [PubMed: 27913612]
7. Popadic Gacesa J, Schick F, Machann J, Grujic N. Intramyocellular lipids and their dynamics assessed by ¹H magnetic resonance spectroscopy. *Clin Physiol Funct Imaging.* 2016
8. Stuart CA, McCurry MP, Marino A, South MA, Howell ME, Layne AS, Ramsey MW, Stone MH. Slow-twitch fiber proportion in skeletal muscle correlates with insulin responsiveness. *J Clin Endocrinol Metab.* 2013; 98:2027–2036. [PubMed: 23515448]
9. Chance B, Im J, Nioka S, Kushmerick M. Skeletal muscle energetics with PNMR: personal views and historic perspectives. *NMR Biomed.* 2006; 19:904–926. [PubMed: 17075955]
10. Kumar V, Chang H, Reiter D, Bradley D, Belury M, McCormack S, Raman S. Phosphorus-31 magnetic resonance spectroscopy: a tool for measuring in vivo mitochondrial oxidative phosphorylation capacity in human skeletal muscle. *J Vis Exp.* 2017; 119
11. Valkovic L, Chmelik M, Krssak M. In-vivo ³¹P-MRS of skeletal muscle and liver: A way for non-invasive assessment of their metabolism. *Anal Biochem.* 2017
12. Kubala E, Munoz-Alvarez KA, Topping G, Hundshammer C, Feuerecker B, Gomez PA, Pariani G, Schilling F, Glaser SJ, Schulte RF, Menzel MI, Schwaiger M. Hyperpolarized ¹³C metabolic magnetic resonance spectroscopy and imaging. *J Vis Exp.* 2016
13. Park JM, Josan S, Mayer D, Hurd RE, Chung Y, Bendahan D, Spielman DM, Jue T. Hyperpolarized ¹³C NMR observation of lactate kinetics in skeletal muscle. *J Exp Biol.* 2015; 218:3308–3318. [PubMed: 26347554]
14. Lindeboom L, Bruls YM, van Ewijk PA, Hesselink MK, Wildberger JE, Schrauwen P, Schrauwen-Hinderling VB. Longitudinal relaxation time editing for acetylcarnitine detection with ¹H-MRS. *Magn Reson Med.* 2017; 77:505–510. [PubMed: 26887359]
15. Young HJ, Jenkins NT, Zhao Q, McCully KK. Measurement of intramuscular fat by muscle echo intensity. *Muscle Nerve.* 2015; 52:963–971. [PubMed: 25787260]
16. Mayans D, Cartwright MS, Walker FO. Neuromuscular ultrasonography: quantifying muscle and nerve measurements. *Phys Med Rehabil Clin N Am.* 2012; 23:133–148, xii. [PubMed: 22239880]
17. Aubrey J, Esfandiari N, Baracos VE, Buteau FA, Frenette J, Putman CT, Mazurak VC. Measurement of skeletal muscle radiation attenuation and basis of its biological variation. *Acta Physiol (Oxf).* 2014; 210:489–497. [PubMed: 24393306]
18. Karampinos DC, Baum T, Nardo L, Alizai H, Yu H, Carballido-Gamio J, Yap SP, Shimakawa A, Link TM, Majumdar S. Characterization of the regional distribution of skeletal muscle adipose

- tissue in type 2 diabetes using chemical shift-based water/fat separation. *J Magn Reson Imaging*. 2012; 35:899–907. [PubMed: 22127958]
19. Chalasani N, Younossi Z, Lavine JE, Diehl AM, Brunt EM, Cusi K, Charlton M, Sanyal AJ. The diagnosis and management of non-alcoholic fatty liver disease: practice Guideline by the American Association for the Study of Liver Diseases, American College of Gastroenterology, and the American Gastroenterological Association. *Hepatology*. 2012; 55:2005–2023. [PubMed: 22488764]
 20. Anstee QM, Targher G, Day CP. Progression of NAFLD to diabetes mellitus, cardiovascular disease or cirrhosis. *Nat Rev Gastroenterol Hepatol*. 2013; 10:330–344. [PubMed: 23507799]
 21. Kasturiratne A, Weerasinghe S, Dassanayake AS, Rajindrajith S, de Silva AP, Kato N, Wickremasinghe AR, de Silva HJ. Influence of non-alcoholic fatty liver disease on the development of diabetes mellitus. *J Gastroenterol Hepatol*. 2013; 28:142–147. [PubMed: 22989165]
 22. Lim S, Oh TJ, Koh KK. Mechanistic link between nonalcoholic fatty liver disease and cardiometabolic disorders. *Int J Cardiol*. 2015; 201:408–414. [PubMed: 26310987]
 23. Valenti L, Bugianesi E, Pajvani U, Targher G. Nonalcoholic fatty liver disease: cause or consequence of type 2 diabetes? *Liver Int*. 2016; 36:1563–1579. [PubMed: 27276701]
 24. Zhang H, Ma Z, Pan L, Xu Y, Shao J, Huang Z, Chen Z, Sun Q, Liu C, Lin M, Yang S, Li X. Hepatic fat content is a determinant of metabolic phenotypes and increased carotid intima-media thickness in obese adults. *Sci Rep*. 2016; 6:21894. [PubMed: 26902311]
 25. Kramer H, Pickhardt PJ, Kliewer MA, Hernando D, Chen GH, Zagzebski JA, Reeder SB. Accuracy of liver fat quantification with advanced CT, MRI, and ultrasound techniques: prospective comparison with MR spectroscopy. *AJR Am J Roentgenol*. 2017; 208:92–100. [PubMed: 27726414]
 26. Castera L, Vilgrain V, Angulo P. Noninvasive evaluation of NAFLD. *Nat Rev Gastroenterol Hepatol*. 2013; 10:666–675. [PubMed: 24061203]
 27. Lamb P, Sahani DV, Fuentes-Orrego JM, Patino M, Ghosh A, Mendonca PR. Stratification of patients with liver fibrosis using dual-energy CT. *IEEE Trans Med Imaging*. 2015; 34:807–815. [PubMed: 25181365]
 28. Loomba R, Wolfson T, Ang B, Hooker J, Behling C, Peterson M, Valasek M, Lin G, Brenner D, Gamst A, Ehman R, Sirlin C. Magnetic resonance elastography predicts advanced fibrosis in patients with nonalcoholic fatty liver disease: a prospective study. *Hepatology*. 2014; 60:1920–1928. [PubMed: 25103310]
 29. Petitclerc L, Sebastiani G, Gilbert G, Cloutier G, Tang A. Liver fibrosis: Review of current imaging and MRI quantification techniques. *J Magn Reson Imaging*. 2017; 45:1276–1295. [PubMed: 27981751]
 30. Levelt E, Pavlides M, Banerjee R, Mahmood M, Kelly C, Sellwood J, Ariga R, Thomas S, Francis J, Rodgers C, Clarke W, Sabharwal N, Antoniadis C, Schneider J, Robson M, Clarke K, Karamitsos T, Rider O, Neubauer S. Ectopic and visceral fat deposition in lean and obese patients with type 2 diabetes. *J Am Coll Cardiol*. 2016; 68:53–63. [PubMed: 27364051]
 31. Hannukainen JC, Guzzardi MA, Virtanen KA, Sanguinetti E, Nuutila P, Iozzo P. Imaging of organ metabolism in obesity and diabetes: treatment perspectives. *Curr Pharm Des*. 2014; 20:6126–6149. [PubMed: 24745922]
 32. Schmid AI, Szendroedi J, Chmelik M, Krssak M, Moser E, Roden M. Liver ATP synthesis is lower and relates to insulin sensitivity in patients with type 2 diabetes. *Diabetes Care*. 2011; 34:448–453. [PubMed: 21216854]
 33. Befroy DE, Perry RJ, Jain N, Dufour S, Cline GW, Trimmer JK, Brosnan J, Rothman DL, Petersen KF, Shulman GI. Direct assessment of hepatic mitochondrial oxidative and anaplerotic fluxes in humans using dynamic ¹³C magnetic resonance spectroscopy. *Nat Med*. 2014; 20:98–102. [PubMed: 24317120]
 34. Matveyenko AV, Butler PC. Relationship between beta-cell mass and diabetes onset. *Diabetes Obes Metab*. 2008; 10(Suppl 4):23–31. [PubMed: 18834430]

35. Lim EL, Hollingsworth KG, Aribisala BS, Chen MJ, Mathers JC, Taylor R. Reversal of type 2 diabetes: normalisation of beta cell function in association with decreased pancreas and liver triacylglycerol. *Diabetologia*. 2011; 54:2506–2514. [PubMed: 21656330]
36. Jodal A, Schibli R, Behe M. Targets and probes for non-invasive imaging of beta-cells. *Eur J Nucl Med Mol Imaging*. 2017; 44:712–727. [PubMed: 28025655]
37. Brom M, Woliner-van der Weg W, Joosten L, Frielink C, Bouckenooghe T, Rijken P, Andralojc K, Goke BJ, de Jong M, Eizirik DL, Behe M, Lahoutte T, Oyen WJ, Tack CJ, Janssen M, Boerman OC, Gotthardt M. Non-invasive quantification of the beta cell mass by SPECT with (1)(1)(1)In-labelled exendin. *Diabetologia*. 2014; 57:950–959. [PubMed: 24488022]
38. Ryden A, Nyman G, Nalin L, Andreasson S, Korsgren O, Eriksson O, Jensen-Waern M. Cardiovascular side-effects and insulin secretion after intravenous administration of radiolabeled Exendin-4 in pigs. *Nucl Med Biol*. 2016; 43:397–402. [PubMed: 27179248]
39. Vinet L, Lamprianou S, Babic A, Lange N, Thorel F, Herrera PL, Montet X, Meda P. Targeting GLP-1 receptors for repeated magnetic resonance imaging differentiates graded losses of pancreatic beta cells in mice. *Diabetologia*. 2015; 58:304–312. [PubMed: 25413047]
40. Badoud F, Perreault M, Zulyniak MA, Mutch DM. Molecular insights into the role of white adipose tissue in metabolically unhealthy normal weight and metabolically healthy obese individuals. *FASEB J*. 2015; 29:748–758. [PubMed: 25411437]
41. Munoz-Garach A, Cornejo-Pareja I, Tinahones FJ. Does metabolically healthy obesity exist? *Nutrients*. 2016; 8
42. Klopfenstein BJ, Kim MS, Krisky CM, Szumowski J, Rooney WD, Purnell JQ. Comparison of 3 T MRI and CT for the measurement of visceral and subcutaneous adipose tissue in humans. *Br J Radiol*. 2012; 85:e826–830. [PubMed: 22514099]
43. Ganesan G, Warren RV, Leproux A, Compton M, Cutler K, Wittkopp S, Tran G, O'Sullivan T, Malik S, Galassetti PR, Tromberg BJ. Diffuse optical spectroscopic imaging of subcutaneous adipose tissue metabolic changes during weight loss. *Int J Obes (Lond)*. 2016; 40:1292–1300. [PubMed: 27089996]
44. Orava J, Nuutila P, Noponen T, Parkkola R, Viljanen T, Enerback S, Rissanen A, Pietilainen KH, Virtanen KA. Blunted metabolic responses to cold and insulin stimulation in brown adipose tissue of obese humans. *Obesity (Silver Spring)*. 2013; 21:2279–2287. [PubMed: 23554353]
45. Madar I, Naor E, Holt D, Ravert H, Dannals R, Wahl R. Brown adipose tissue response dynamics: in vivo insights with the voltage sensor 18F-fluorobenzyl triphenyl phosphonium. *PLoS One*. 2015; 10:e0129627. [PubMed: 26053485]
46. Franssens BT, Hoogduin H, Leiner T, van der Graaf Y, Visseren FL. Relation between brown adipose tissue and measures of obesity and metabolic dysfunction in patients with cardiovascular disease. *J Magn Reson Imaging*. 2017
47. De Boer MP, Meijer RI, Wijnstok NJ, Jonk AM, Houben AJ, Stehouwer CD, Smulders YM, Eringa EC, Serne EH. Microvascular dysfunction: a potential mechanism in the pathogenesis of obesity-associated insulin resistance and hypertension. *Microcirculation*. 2012; 19:5–18. [PubMed: 21883642]
48. Sorop O, Olver TD, van de Wouw J, Heinonen I, van Duin RW, Duncker DJ, Merkus D. The microcirculation: a key player in obesity-associated cardiovascular disease. *Cardiovasc Res*. 2017
49. Cheung CY, Ikram MK, Klein R, Wong TY. The clinical implications of recent studies on the structure and function of the retinal microvasculature in diabetes. *Diabetologia*. 2015; 58:871–885. [PubMed: 25669631]
50. Camici PG, d'Amati G, Rimoldi O. Coronary microvascular dysfunction: mechanisms and functional assessment. *Nat Rev Cardiol*. 2015; 12:48–62. [PubMed: 25311229]
51. Lanting SM, Johnson NA, Baker MK, Caterson ID, Chuter VH. The effect of exercise training on cutaneous microvascular reactivity: A systematic review and meta-analysis. *J Sci Med Sport*. 2017; 20:170–177. [PubMed: 27476375]
52. Eriksson S, Nilsson J, Stureson C. Non-invasive imaging of microcirculation: a technology review. *Med Devices (Auckl)*. 2014; 7:445–452. [PubMed: 25525397]

53. Meijer RI, De Boer MP, Groen MR, Eringa EC, Rattigan S, Barrett EJ, Smulders YM, Serne EH. Insulin-induced microvascular recruitment in skin and muscle are related and both are associated with whole-body glucose uptake. *Microcirculation*. 2012; 19:494–500. [PubMed: 22360160]
54. Sorensen BM, Houben AJ, Berendschot TT, Schouten JS, Kroon AA, van der Kallen CJ, Henry RM, Koster A, Sep SJ, Dagnelie PC, Schaper NC, Schram MT, Stehouwer CD. Prediabetes and type 2 diabetes are associated with generalized microvascular dysfunction: the Maastricht study. *Circulation*. 2016; 134:1339–1352. [PubMed: 27678264]
55. Lanza GA, Camici PG, Galiuto L, Niccoli G, Pizzi C, Di Monaco A, Sestito A, Novo S, Piscione F, Tritto I, Ambrosio G, Bugiardini R, Crea F, Marzilli M, Gruppo di Studio di Fisiopatologia Coronarica e Microcircolazione SidC. Methods to investigate coronary microvascular function in clinical practice. *J Cardiovasc Med (Hagerstown)*. 2013; 14:1–18. [PubMed: 23222188]
56. von Scholten BJ, Hasbak P, Christensen TE, Ghotbi AA, Kjaer A, Rossing P, Hansen TW. Cardiac (82)Rb PET/CT for fast and non-invasive assessment of microvascular function and structure in asymptomatic patients with type 2 diabetes. *Diabetologia*. 2016; 59:371–378. [PubMed: 26526662]
57. Aroor AR, Mandavia CH, Sowers JR. Insulin resistance and heart failure: molecular mechanisms. *Heart Fail Clin*. 2012; 8:609–617. [PubMed: 22999243]
58. Banerjee P, Motiwala A, Mustafa HM, Gani MA, Fourali S, Ali D. Does left ventricular diastolic dysfunction progress through stages? Insights from a community heart failure study. *Int J Cardiol*. 2016; 221:850–854. [PubMed: 27434359]
59. Nagueh SF, Smiseth OA, Appleton CP, Byrd BF 3rd, Dokainish H, Edvardsen T, Flachskampf FA, Gillebert TC, Klein AL, Lancellotti P, Marino P, Oh JK, Popescu BA, Waggoner AD. Recommendations for the evaluation of left ventricular diastolic function by echocardiography: an update from the American Society of Echocardiography and the European Association of Cardiovascular Imaging. *J Am Soc Echocardiogr*. 2016; 29:277–314. [PubMed: 27037982]
60. Dugo C, Rigolli M, Rossi A, Whalley GA. Assessment and impact of diastolic function by echocardiography in elderly patients. *J Geriatr Cardiol*. 2016; 13:252–260. [PubMed: 27103921]
61. Wei J, Nelson MD, Szczepaniak EW, Smith L, Mehta PK, Thomson LE, Berman DS, Li D, Bairey Merz CN, Szczepaniak LS. Myocardial steatosis as a possible mechanistic link between diastolic dysfunction and coronary microvascular dysfunction in women. *Am J Physiol Heart Circ Physiol*. 2016; 310:H14–19. [PubMed: 26519031]
62. Rider OJ, Francis JM, Tyler D, Byrne J, Clarke K, Neubauer S. Effects of weight loss on myocardial energetics and diastolic function in obesity. *Int J Cardiovasc Imaging*. 2013; 29:1043–1050. [PubMed: 23269470]
63. Le Page LM, Rider OJ, Lewis AJ, Ball V, Clarke K, Johansson E, Carr CA, Heather LC, Tyler DJ. Increasing pyruvate dehydrogenase flux as a treatment for diabetic cardiomyopathy: a combined ¹³C hyperpolarized magnetic resonance and echocardiography study. *Diabetes*. 2015; 64:2735–2743. [PubMed: 25795215]
64. Lewis AJ, Miller JJ, McCallum C, Rider OJ, Neubauer S, Heather LC, Tyler DJ. Assessment of metformin-induced changes in cardiac and hepatic redox state using hyperpolarized[1-¹³C]pyruvate. *Diabetes*. 2016; 65:3544–3551. [PubMed: 27561726]
65. Moberly SP, Mather KJ, Berwick ZC, Owen MK, Goodwill AG, Casalini ED, Hutchins GD, Green MA, Ng Y, Considine RV, Perry KM, Chisholm RL, Tune JD. Impaired cardiometabolic responses to glucagon-like peptide 1 in obesity and type 2 diabetes mellitus. *Basic Res Cardiol*. 2013; 108:365. [PubMed: 23764734]
66. Scheuermann-Freestone M, Madsen PL, Manners D, Blamire AM, Buckingham RE, Styles P, Radda GK, Neubauer S, Clarke K. Abnormal cardiac and skeletal muscle energy metabolism in patients with type 2 diabetes. *Circulation*. 2003; 107:3040–3046. [PubMed: 12810608]
67. Gallagher D, Kelley DE, Thornton J, Boxt L, Pi-Sunyer X, Lipkin E, Nyenwe E, Janumala I, Heshka S, Group MRIASGotLAR. Changes in skeletal muscle and organ size after a weight-loss intervention in overweight and obese type 2 diabetic patients. *Am J Clin Nutr*. 2017; 105:78–84. [PubMed: 27881389]
68. van der Meer RW, Rijzewijk LJ, de Jong HW, Lamb HJ, Lubberink M, Romijn JA, Bax JJ, de Roos A, Kamp O, Paulus WJ, Heine RJ, Lammertsma AA, Smit JW, Diamant M. Pioglitazone improves cardiac function and alters myocardial substrate metabolism without affecting cardiac triglyceride

- accumulation and high-energy phosphate metabolism in patients with well-controlled type 2 diabetes mellitus. *Circulation*. 2009; 119:2069–2077. [PubMed: 19349323]
69. Zheng J, An H, Coggan AR, Zhang X, Bashir A, Muccigrosso D, Peterson LR, Gropler RJ. Noncontrast skeletal muscle oximetry. *Magn Reson Med*. 2014; 71:318–325. [PubMed: 23424006]
70. Garcovich M, Veraldi S, Di Stasio E, Zocco MA, Monti L, Toma P, Pompili M, Gasbarrini A, Nobili V. Liver stiffness in pediatric patients with fatty liver disease: diagnostic accuracy and reproducibility of shear-wave elastography. *Radiology*. 2017; 283:820–827. [PubMed: 27982761]
71. Nirengi S, Homma T, Inoue N, Sato H, Yoneshiro T, Matsushita M, Kameya T, Sugie H, Tsuzaki K, Saito M, Sakane N, Kurosawa Y, Hamaoka T. Assessment of human brown adipose tissue density during daily ingestion of thermogenic capsinoids using near-infrared time-resolved spectroscopy. *J Biomed Opt*. 2016; 21:091305. [PubMed: 27135066]
72. Enfield J, McGrath J, Daly SM, Leahy M. Enhanced in vivo visualization of the microcirculation by topical application of fructose solution confirmed with correlation mapping optical coherence tomography. *J Biomed Opt*. 2016; 21:081212. [PubMed: 27311423]
73. Haris M, Singh A, Cai K, Kogan F, McGarvey J, Debrosse C, Zsido GA, Witschey WR, Koomalsingh K, Pilla JJ, Chirinos JA, Ferrari VA, Gorman JH, Hariharan H, Gorman RC, Reddy R. A technique for in vivo mapping of myocardial creatine kinase metabolism. *Nat Med*. 2014; 20:209–214. [PubMed: 24412924]

**Figure.**

The cardiac consequences of cardiometabolic disease ensue from functional and structural alterations in multiple organ systems, including skeletal muscle, liver, the pancreas and microcirculation. Primary imaging targets for non-invasive investigation of CMD are listed. Multiple imaging modalities are used in the evaluation of organ systems involved in CMD. Skeletal muscle investigation typically involves multinuclear MR spectroscopy and MR imaging. Liver is non-invasively interrogated using CT, elastography (both MR and US) and PET for fat quantification, fibrosis quantification and glucose utilization, respectively. Pancreatic beta cell deficit is measured in humans using novel SPECT and PET techniques and in preclinical models with magnetic nanoparticles and MR imaging techniques. Adipose tissue can be quantified using MRI, CT, US and dual-energy x-ray absorptiometry. Brown adipose tissue can be quantified using FDG-PET techniques. Microcirculatory rarefaction and resistance can be evaluated with optical imaging techniques and PET. Finally, the heart in CMD can be investigated using US, MRI and multinuclear MR spectroscopy.